MARTIN MARIETTA ENERGY SYSTEMS LIBRARIES

3 4456 0334894 6

ORNL/TM-11623

OAK RIDGE NATIONAL LABORATORY

MARTIN MARIETTA

Characteristics of Edge Plasma Turbulence on the ATF Torsatron

T. Uckan
C. Hidalgo
J. D. Bell
J. H. Harris
J. L. Dunlap
J. B. Wilgen
Ch. P. Ritz
T. L. Rhodes
A. J. Wootton

OAK RIDGE NATIONAL LABORATORY
CENTRAL RESEARCH LIBRARY
CIRCULATION SECTION
4500N ROOM 175
LIBRARY LOAN COPY
DO NOT TRANSFER TO ANOTHER PERSON
If you wish someone else to see this report, send in name with report and the library will arrange a loan.

MANAGED BY
MARTIN MARIETTA ENERGY SYSTEMS, INC.
FOR THE UNITED STATES
DEPARTMENT OF ENERGY

This report has been reproduced directly from the best available copy.

Available to DOE and DOE contractors from the Office of Scientific and Technical Information, P.O. Box 62, Oak Ridge, TN 37831; prices available from (615) 576-8401, FTS 626-8401.

Available to the public from the National Technical Information Service, U.S. Department of Commerce, 5285 Port Royal Road, Springfield, VA 22161.

This report was prepared as an account of work sponsored by an agency of the United States Government. Neither the United States Government nor any agency thereof, nor any of their employees, makes any warranty, express or implied, or assumes any legal liability or responsibility for the accuracy, completeness, or usefulness of any information, apparatus, product, or process disclosed, or represents that its use would not infringe privately owned rights. Reference herein to any specific commercial product, process, or service by trade name, trademark, manufacturer, or otherwise, does not necessarily constitute or imply its endorsement, recommendation, or favoring by the United States Government or any agency thereof. The views and opinions of authors expressed herein do not necessarily state or reflect those of the United States Government or any agency thereof.

ORNL/TM-11623
Dist. Category UC-426

Fusion Energy Division

CHARACTERISTICS OF EDGE PLASMA TURBULENCE ON THE ATF TORSATRON

T. Uckan
C. Hidalgo*
J. D. Bell
J. H. Harris
J. L. Dunlap
J. B. Wilgen

Ch. P. Ritz
T. L. Rhodes
A. J. Wootton
Fusion Research Center, The University of Texas, Austin

*Permanent address: Asociación EURATOM/CIEMAT, Madrid, Spain.

Date published: March 1991

Prepared for the
Office of Fusion Energy
under Budget Activity No. AT 10 10 15 B

Prepared by
OAK RIDGE NATIONAL LABORATORY
Oak Ridge, Tennessee 37831-6285
managed by
MARTIN MARIETTA ENERGY SYSTEMS, INC.
for the
U.S. DEPARTMENT OF ENERGY
under contract DE-AC05-84OR21400

MARTIN MARIETTA ENERGY SYSTEMS LIBRARIES

3 4456 0334894 6

CONTENTS

ABSTRACT v
I. INTRODUCTION 1
II. EXPERIMENTAL SETUP AND ANALYSIS TECHNIQUES 1
III. EXPERIMENTAL OBSERVATIONS AND DISCUSSIONS 5
IV. CONCLUSION 13
ACKNOWLEDGMENTS 15
REFERENCES 17

ABSTRACT

Measurements of electrostatic fluctuations on the edge of the Advanced Toroidal Facility (ATF) torsatron [J. F. Lyon et al., Fusion Technol. **10**, 179 (1986)] are used to study the role of the edge turbulence in the particle transport in this current-free magnetic configuration. Spatial profiles of the plasma electron density n_e, temperature T_e, and fluctuations in density ($\tilde{n}_e$) and in the plasma floating potential ($\tilde{\phi}_f$) are measured at the edge in electron cyclotron heated plasmas using a Langmuir probe array. At the last closed flux surface (LCFS), $r/a \approx 1$, $T_e \approx 20$–40 eV, and $n_e \approx 10^{12}\,\mathrm{cm}^{-3}$ for a line-averaged electron density $\bar{n}_e = (3\text{–}6) \times 10^{12}\,\mathrm{cm}^{-3}$. The relative fluctuation levels decrease as the probe is moved into the core plasma. For $T_e > 20$ eV, $\tilde{n}_e/n_e \approx 5\%$, and $e\tilde{\phi}_f/T_e \approx 2\tilde{n}_e/n_e$ at $r/a = 0.95$. The measured fluctuation spectra are broadband (40–300 kHz) with $\bar{k}\rho_s \approx 0.05$–$0.1$, where $\bar{k}$ is the average wave number of the fluctuations and ρ_s is the ion Larmor radius at the sound speed. Near the LCFS, the density fluctuations can be approximated by $\tilde{n}_e/n_e \approx 0.4/\bar{k}L_n$, where L_n is the gradient scale length of n_e. The propagation direction of the fluctuations reverses to the electron diamagnetic direction at $r/a < 1$. The phase velocity of the fluctuations and the electron drift velocity are comparable. The particle flux estimated from the fluctuations is consistent with fluxes obtained from the particle balance using the H_α spectroscopic measurements. Many of the features seen in the ATF edge fluctuations resemble those of ohmically heated plasmas in the Texas Experimental Tokamak (TEXT) [Ch. P. Ritz et al., Phys. Rev. Lett. **62**, 1844 (1989)].

I. INTRODUCTION

The anomalous energy transport and particle transport in tokamaks and stellarators are observed to have similar dependences on plasma parameters.[1] The basic mechanisms responsible for this anomaly are the subject of ongoing research in fusion devices. Investigations of edge turbulence[2] in different magnetic configurations can help to identify the underlying physical processes responsible for this anomalous plasma cross-field transport. To understand the driving forces on the edge fluctuations in terms of the plasma current and the magnetic configuration, recent measurements of electrostatic turbulence in ohmically heated plasmas at the edge of the Texas Experimental Tokamak[3] (TEXT) have been extended to the current-free Advanced Toroidal Facility[4] (ATF) torsatron. The TEXT results show that electrostatic fluctuations are the dominant mechanism for energy and particle transport in the edge.[3,5] Initial electrostatic fluctuation measurements on ATF have been carried out at the edge with a fast reciprocating Langmuir probe (FRLP) array[6] similar to the one used in the TEXT experiments.

The paper is organized as follows: The experimental setup and the data analysis methods are described in Sec. II. In Sec. III, measurements of plasma electron density n_e, electron temperature T_e, and fluctuations in density ($\tilde{n}_e$) and plasma floating potential ($\tilde{\phi}_f$) at the edge of ATF in electron cyclotron heated (ECH) plasmas are presented and their turbulence characteristics are discussed. Brief conclusions follow in Sec. IV.

II. EXPERIMENTAL SETUP AND ANALYSIS TECHNIQUES

The ATF torsatron has a stellarator configuration of poloidal multipolarity $l = 2$, 12 field periods ($M = 12$), a major radius $R_0 = 2.1$ m, and an average plasma radius a = 0.27 m. The current-free magnetic configuration of ATF is produced by external means with a moderate shear: The rotational transform ($\iota = \iota/2\pi = 1/q$, where q is the safety factor) at the last closed flux surface (LCFS) is $\iota \approx 1$, which is about a factor of 3 higher than the central value. Initial fluctuation measurements at the ATF edge have been carried out around the LCFS, $r/a \approx 1$, where r is the average radial coordinate, with the FRLP in ECH plasmas at a magnetic field B = 0.95 T. These plasmas were created using a 53-GHz gyrotron source with heating power P = 200 kW. In these ECH plasmas, a representative range for the line-averaged plasma density is $\bar{n}_e = (3\text{–}6) \times 10^{12}$ cm^{-3}, and the plasma stored energy $W_p \approx 1\text{–}2$ kJ.

The Langmuir probe array is located one field period (30° in toroidal angle) away from the instrumented rail limiter.[7] The probe is inserted into the edge plasma from the top, as indicated in Fig. 1, moves 5 cm into the plasma in 50 ms, and remains there for about 60 ms to carry out the fluctuation measurements as shown in Fig. 2. The measure-

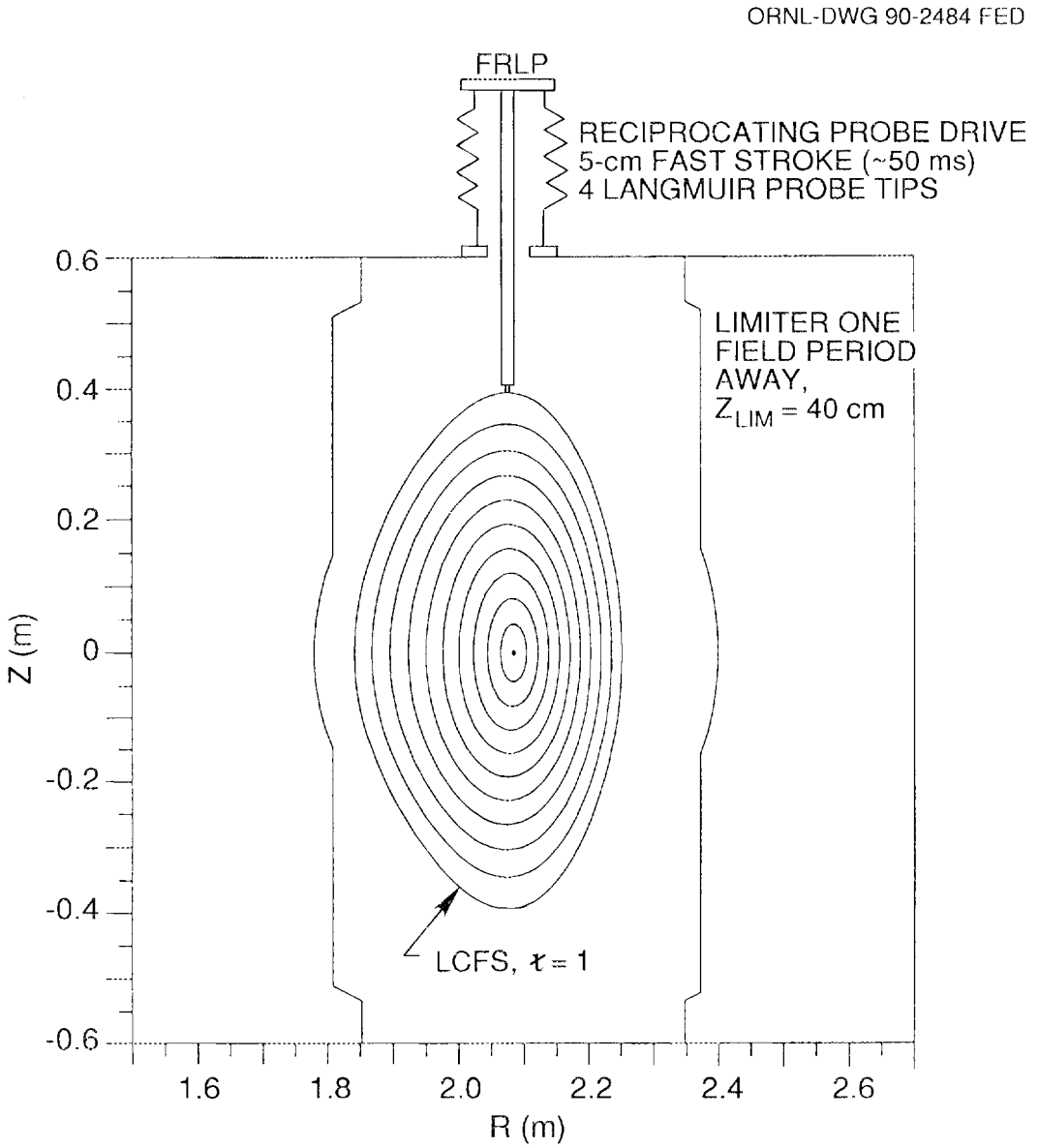

Fig. 1. Constant flux surfaces and the location of the FRLP on ATF. The rotational transform is $\iota = \iota/2\pi \approx 1$ at the LCFS, which the FRLP contacts at $Z_{LCFS} = 0.4$ m. The rail limiter is located one field period (30° in toroidal angle) away from the FRLP and is positioned at $Z_{LIM} = 0.4$ m.

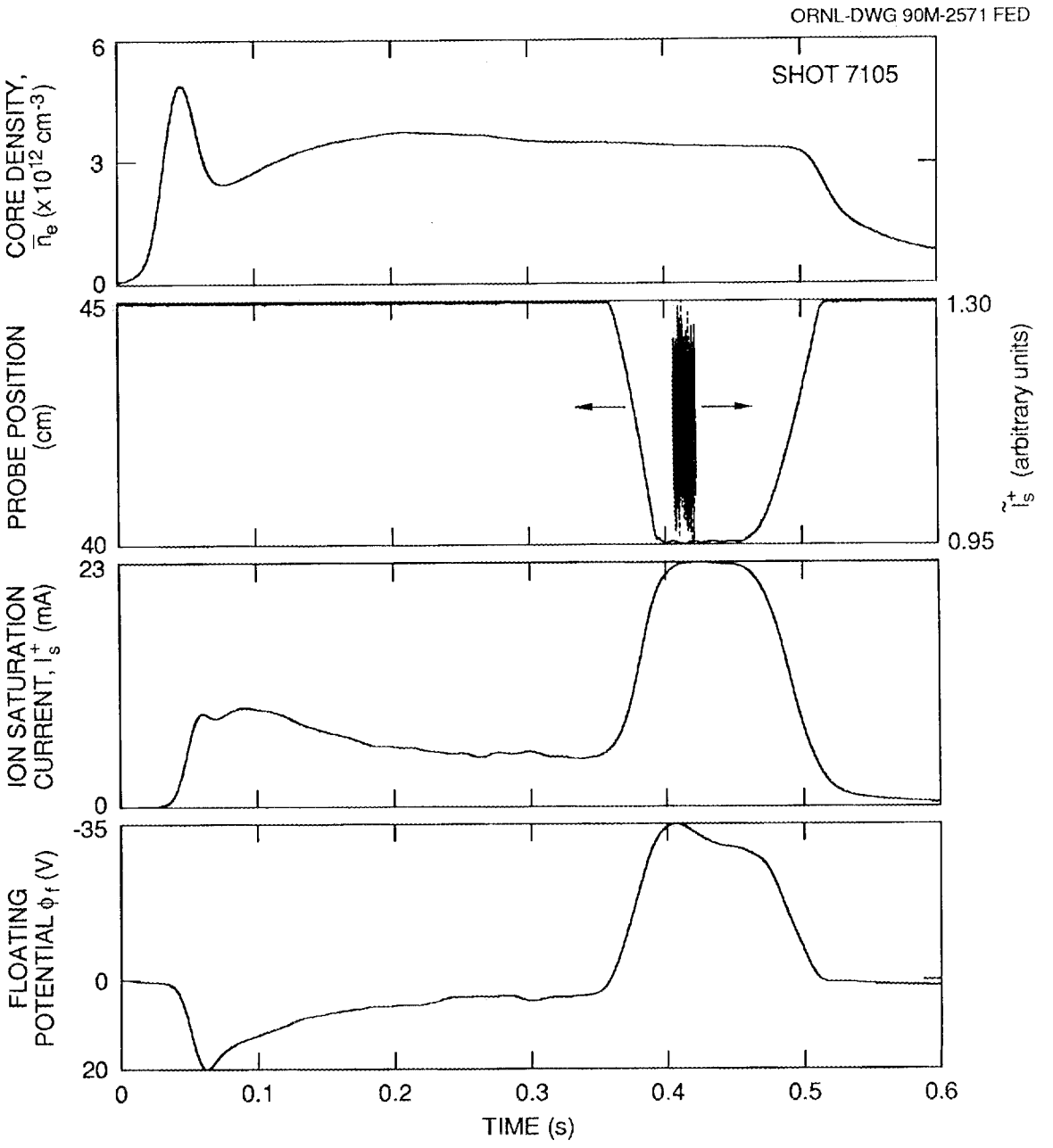

Fig. 2. Time evolution of the line-averaged core plasma density $\bar{n}_e$; the FRLP position, which is started from vertical at Z = 0.45 m and goes inward to Z_{LCFS} = 0.4 m in about 50 ms; the ion saturation current $I_s^+ \sim n_e T_e^{0.5}$ and its fluctuations $\tilde{I}_s^+ \sim \tilde{n}_e$ since $\tilde{T}_e$ is ignored; and the plasma floating potential ϕ_f. The fluctuation parameters are measured when the probe is stationary (~60 ms) before it retracts to its original position.

ments are made during the steady-state phase of the plasma discharge, and the hard x-ray measurements indicate no evidence of tail electrons from the ECH that might affect the probe measurements. The probe head consists of a square array of four tips, 0.5 mm in diameter, that are 2 mm long and 2 mm apart. The two tips that are aligned perpendicular to the local magnetic field operate as a double Langmuir probe to measure the edge plasma n_e, T_e, and $\tilde{n}_e/n_e$ profiles inside (about 2 cm, where $r/a \approx 0.95$ and $\iota \approx 0.85$) and outside (where $r/a \approx 1.15$) the LCFS. These profiles are obtained continuously in space while the FRLP moves into the core plasma as shown in Fig. 2. The other two tips are used to measure the plasma floating potential ϕ_f, its fluctuations $\tilde{\phi}_f$, and the wave number k perpendicular to the local magnetic field. The fluctuation signals are digitized at 1 MHz for about 16 ms and low-pass filtered at 0.4 MHz to prevent aliasing. Then the data are analyzed with spectral analysis techniques[8] by using fast Fourier transform to obtain their power spectrum $S(k,\omega)$ as a function of frequency ω and k from the two-probe technique described in Ref. 9. Ensemble averaging of the spectral distribution of the flux $\tilde{\Gamma}_{\tilde{n}\tilde{\phi}}(\omega)$, obtained from the correlation of density and plasma potential fluctuations ($\tilde{\phi}_p$), gives the fluctuation-induced radial particle flux:

$$\tilde{\Gamma}_{\tilde{n}\tilde{\phi}} = \langle \tilde{n}_e \tilde{v}_r \rangle = 2 \Sigma_{\omega>0} \tilde{\Gamma}_{\tilde{n}\tilde{\phi}}(\omega), \tag{1}$$

where $\tilde{v}_r = -ik\tilde{\phi}_p/B$ is the radial velocity resulting from the $\tilde{E} \times B$ convection of the fluctuating electric field $\tilde{E}$ measured across the probe tips that are perpendicular to the local magnetic field. The frequency-resolved flux is estimated from many independent realizations using a triple correlation technique:[10]

$$\tilde{\Gamma}_{\tilde{n}\tilde{\phi}}(\omega) = \mathrm{Re}[\langle -ik(\omega)\tilde{n}_e^*(\omega)\tilde{\phi}_p(\omega)\rangle]/B. \tag{2}$$

Further, to understand the physical process better, $\tilde{\Gamma}_{\tilde{n}\tilde{\phi}}(\omega)$ can be expressed as[8]

$$\Gamma_{\tilde{n}\tilde{\phi}}(\omega) \approx (k/B)\gamma_{\tilde{n}\tilde{\phi}}\, \tilde{n}_{rms}\, \tilde{\phi}_{rms} \sin \theta_{\tilde{n}\tilde{\phi}}, \tag{3}$$

where $\gamma_{\tilde{n}\tilde{\phi}}$ is the coherence, $\theta_{\tilde{n}\tilde{\phi}}$ is the phase angle between the density and plasma potential fluctuations, and $\tilde{n}_{rms}$ and $\tilde{\phi}_{rms}$ are the rms values of the density and the plasma potential fluctuations obtained from their auto-power spectra, respectively.

III. EXPERIMENTAL OBSERVATIONS AND DISCUSSIONS

The spatial profiles of the edge plasma density, the electron temperature, and the plasma floating potential are given in Fig. 3 for $0.95 < r/a < 1.15$. Near the LCFS, at $r/a \approx 1$, the typical ECH edge plasma parameters are $n_e = (1\text{–}1.2) \times 10^{12}$ cm^{-3} and $T_e = 30\text{–}40$ eV. The characteristic e-folding density and temperature scale lengths are $L_n = [-(1/n_e)(dn_e/dr)]^{-1} \approx 3\text{–}4$ cm and $L_T > 2L_n$, respectively. These values are comparable to those for ohmically heated plasmas in TEXT at 2 T, as discussed in Ref. 3. The plasma potential ϕ_p can be estimated from ϕ_f and T_e as $\phi_p \approx \phi_f + \delta_p T_e$, where δ_p is given as[11] $\delta_p = -0.5 \times \ln[2\pi\mu(1 + T_i/T_e)(1 - \gamma_s)^{-2}]$, which depends on the probe material, the heat load on the probe, the ion temperature T_i, the species mass ratio $\mu = m_e/m_i$, and the secondary electron emission coefficient γ_s. Typically, $\delta_p \approx 1\text{–}3$ for hydrogen plasmas;[11] for this study $\delta_p = 2.5$ is used, corresponding to $T_i/T_e \approx 1$ and $\gamma_s \approx 0$.

The edge profiles of the normalized density ($\tilde{n}_e/n_e$) and potential ($\tilde{\phi}_f/T_e$) fluctuations are given in Fig. 4. Their typical values at $r/a \approx 1$ are $\tilde{n}_e/n_e \approx 0.05\text{–}0.1$ and $\tilde{\phi}_f/T_e \approx 0.1\text{–}0.2$, which are lower than those in TEXT plasmas.[3] The relative levels of these fluctuations decrease as the probe is moved into the core plasma, where $T_e > 20$ eV and $\tilde{\phi}_f/T_e \approx 2\tilde{n}_e/n_e$ at $r/a \approx 0.95$.

In Fig. 5 the variation of the estimated mean value of the wave number in the edge is shown. The range of values is $\bar{k} = 1\text{–}3$ cm^{-1}; thus, $\bar{k}\rho_s \approx 0.05\text{–}0.1$, where ρ_s is the ion Larmor radius at the sound speed. Near the LCFS, the relative density fluctuations may be closely approximated by $\tilde{n}_e/n_e \approx 0.4/\bar{k}L_n \approx 4\rho_s/L_n$, as predicted for the drift wave description of the edge plasma turbulence.[12] The sign change observed on the wave number in the edge (Fig. 5) indicates that the propagation direction of the fluctuations is in the direction of the ion diamagnetic drift for $r/a > 1$, but it reverses to the electron diamagnetic drift direction for $r/a < 1$. Similar results are observed on the TEXT tokamak.[2,3]

Fluctuation spectra of $\tilde{n}_e$ and $\tilde{\phi}_f$ have been examined for frequencies up to 400 kHz. In Fig. 6 the integrated potential fluctuation power spectra $S(\omega)$ and $S(k)$ are shown. The power spectrum $S(\omega)$ is broadband, Fig. 6(a), and mostly in the range 40–300 kHz. For large values of $\omega/2\pi$ (>200 kHz) and k, the power spectra can be represented by $S(\omega) \sim \omega^{-\alpha_\omega}$ and $S(k) \sim k^{-\alpha_k}$, where $\alpha_\omega \approx \alpha_k \approx 4 \pm 1$. The general shape of the $\tilde{n}_e$ power spectrum is also similar to that of $\tilde{\phi}_f$. The shape of $S(k)$ may not be its true shape.[13] However, the technique used here[9] provides a reliable determination of $\bar{k}$ and the spectral width σ_k, which is the rms deviation about $\bar{k}$, as discussed in Ref. 13. The wave number spectrum analysis indicates that inside the LCFS σ_k decreases with increasing local electron temperature, as shown in Fig. 7. Thus the correlation length $L_c = 1/\sigma_k$ increases with

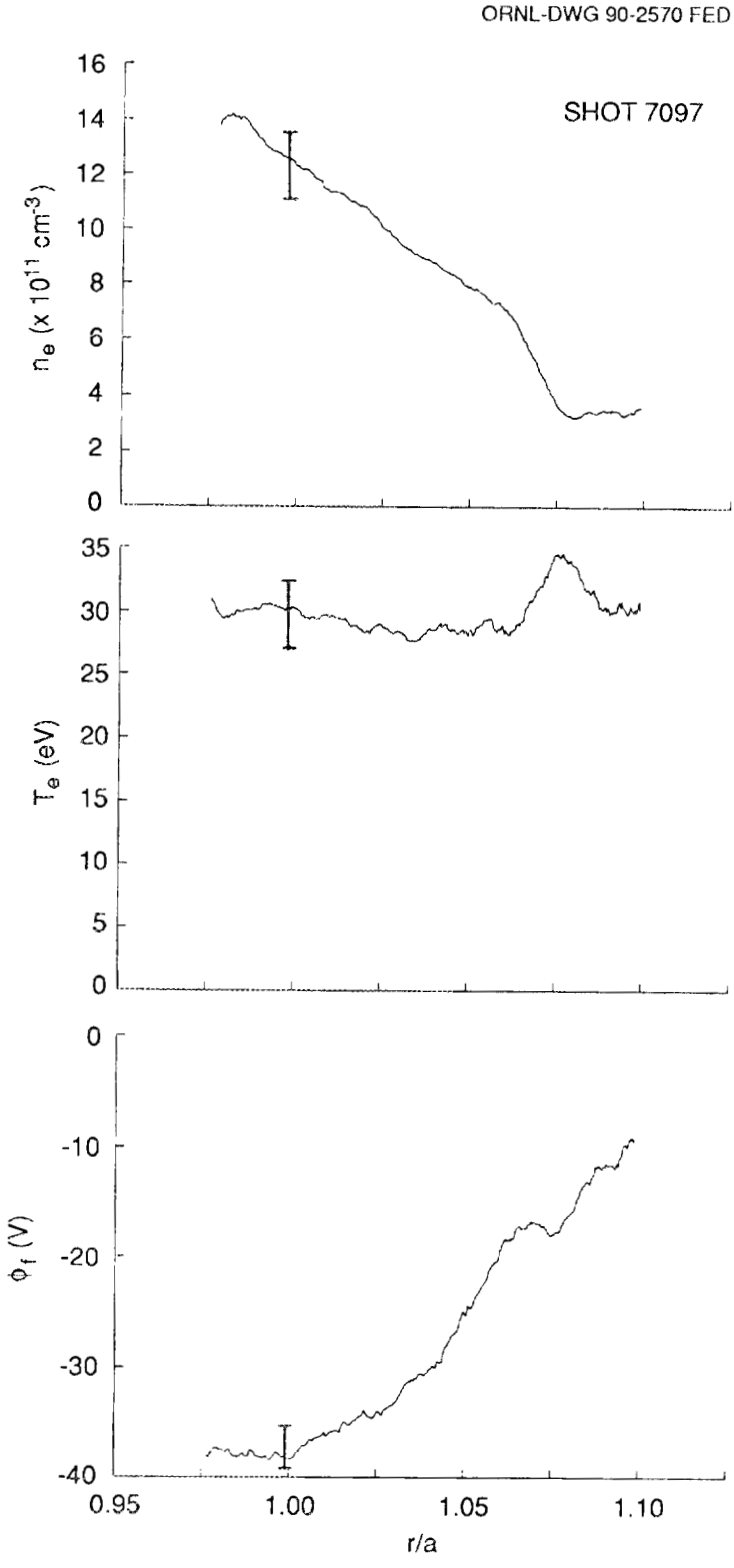

Fig. 3. Edge plasma electron density, electron temperature, and floating potential profiles for ECH plasmas in ATF.

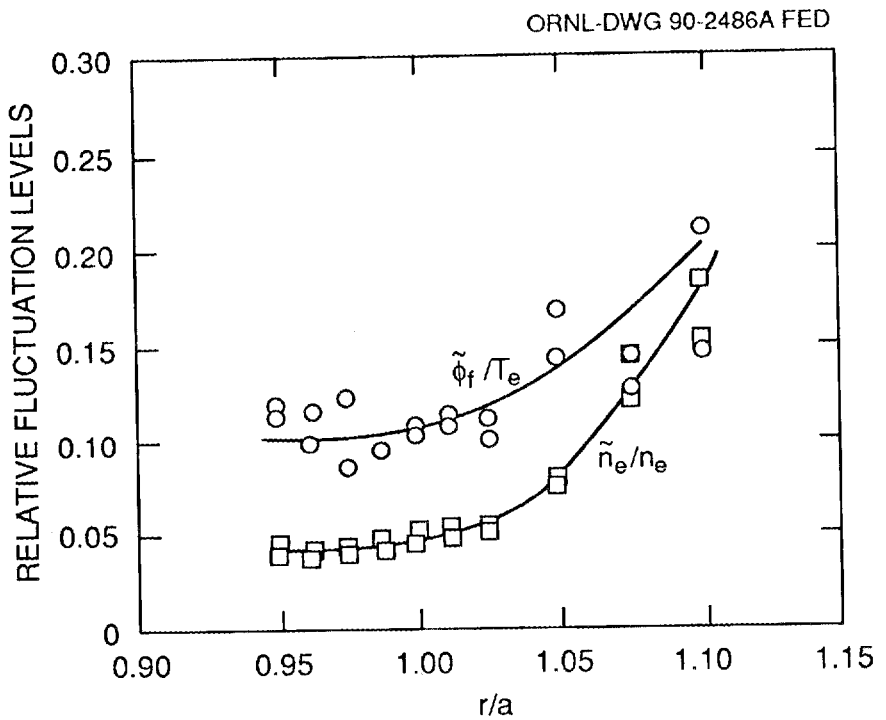

Fig. 4. Relative fluctuation levels for edge density (squares) and potential (circles). Associated errors in ($\tilde{n}_e/n_e$) and ($\tilde{\phi}_f/T_e$) are ~25%.

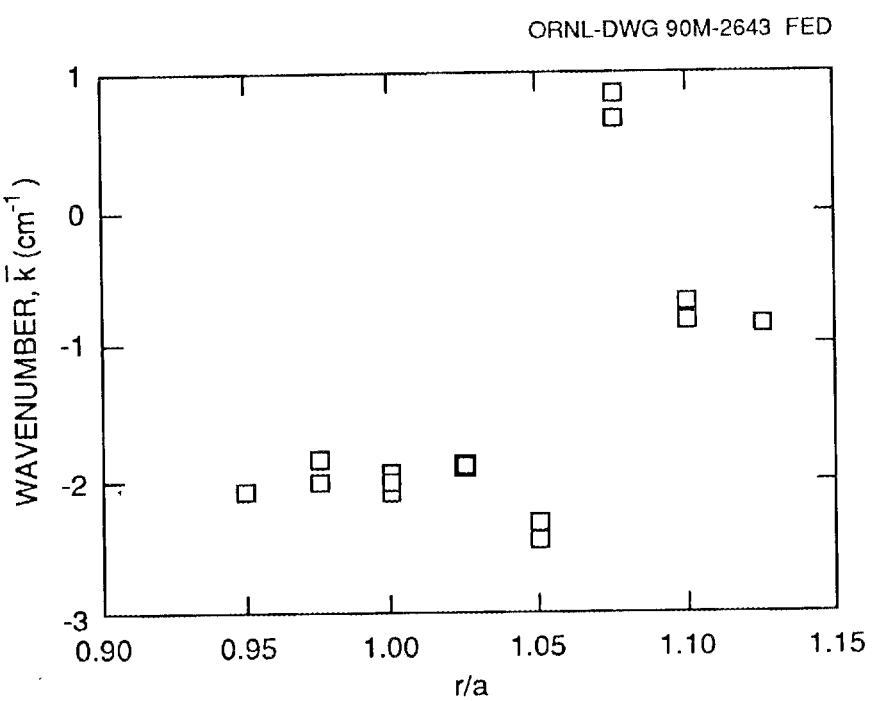

Fig. 5. Variations of the average wave number $\bar{k}$ in the edge.

ORNL-DWG 90-2531AR FED

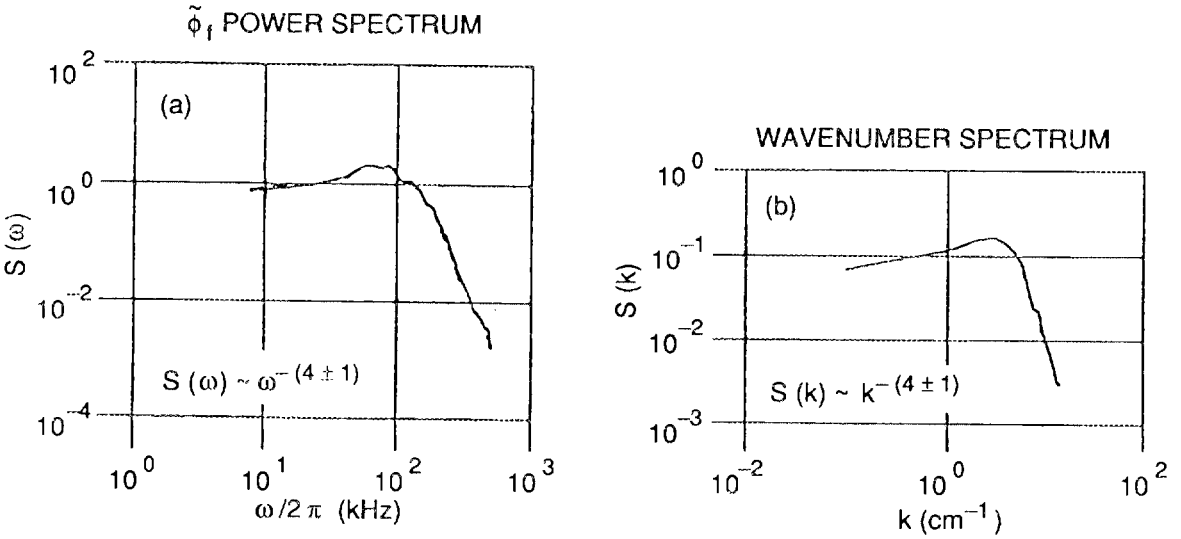

Fig. 6. (a) Power spectrum S(ω) of the potential fluctuations. (b) Wave number spectrum S(k).

ORNL-DWG 90M-2533R FED

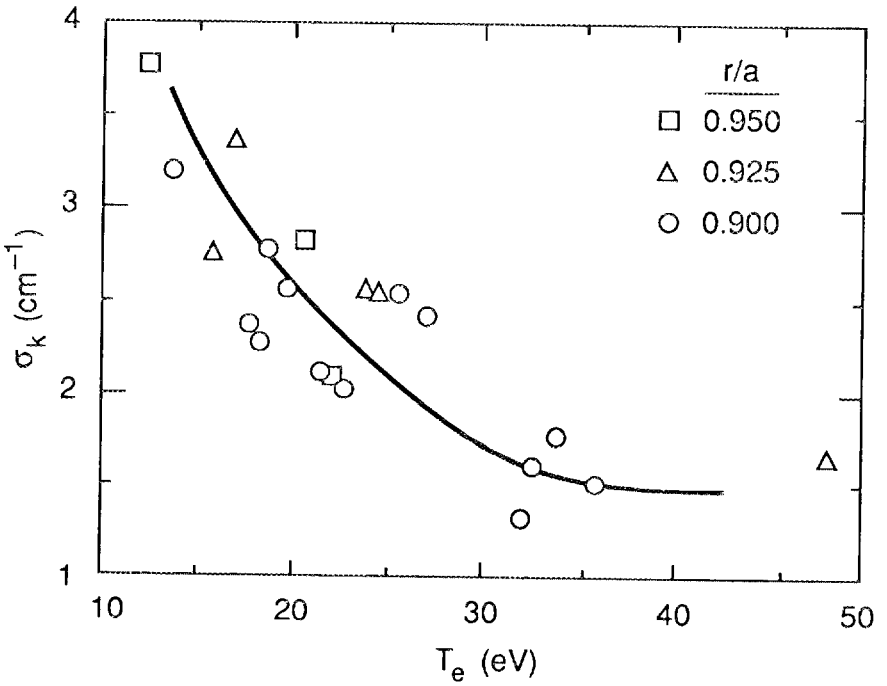

Fig. 7. Variations of spectral width σ_k with T_e inside the LCFS.

temperature;[14] typically $L_c \approx 1$ cm, which is much larger than the probe tip separation, for $T_e > 35$ eV.

As a simple first estimate, the fluctuation-induced particle flux is calculated from Eqs. (1) and (2) by taking $\tilde{\phi}_p \approx \tilde{\phi}_f$, i.e., by neglecting the contribution of the electron temperature fluctuations $\tilde{T}_e$ to $\tilde{\phi}_p$ $[= (\tilde{\phi}_f^2 + \delta_p^2 \tilde{T}_e^2 + 2\delta_p \langle \tilde{\phi}_f \tilde{T}_e \rangle)^{0.5}]$. The correlation between $\tilde{\phi}_f$ and $\tilde{T}_e$ in ATF has not yet been determined, and there is uncertainty concerning the level of $\tilde{T}_e$: Outside the LCFS, $\tilde{T}_e/T_e$ has been observed to be smaller than $\tilde{n}_e/n_e$,[14,15] whereas around the LCFS in ATF the upper bound of $\tilde{T}_e/T_e$ may be comparable to $\tilde{n}_e/n_e$,[14] as shown in Fig. 8. This initial estimate of $\tilde{T}_e/T_e$ is obtained from the so-called triple Langmuir probe technique;[14] the associated error may be large because of possible contributions from the fluctuating electric field between the probe tips. At the LCFS, where $\Gamma_{\tilde{n}\tilde{\phi}}$ will be compared with the global particle flux later, the inclusion of $\tilde{T}_e$ could increase the particle flux by a factor of ~2 as the result of assuming positive correlation between $\tilde{\phi}_f$ and $\tilde{T}_e$ and using $\tilde{T}_e/\tilde{\phi}_f \approx 0.75$ at $r/a \approx 1$ from the measurements (Fig. 9) to estimate $\tilde{\phi}_p$ in Eq. (2).

As shown in Fig. 10, the correlation between the density and the floating potential fluctuations is high, $\gamma_{\tilde{n}\tilde{\phi}} \approx 0.8$, up to 150 kHz, and beyond 250 kHz it drops to ~0.2. The corresponding phase angle is $\theta_{\tilde{n}\tilde{\phi}} \approx 70°$ around 150 kHz. The frequency-resolved particle flux $\Gamma_{\tilde{n}\tilde{\phi}}(\omega)$ is dominated by frequency components below 250 kHz (Fig. 10) and reaches a maximum at 100–150 kHz, where the phase angle has its maximum. The spatial edge profile of the fluctuation-induced particle flux $\Gamma_{\tilde{n}\tilde{\phi}}$, which is obtained from the sum of $\Gamma_{\tilde{n}\tilde{\phi}}(\omega)$ over the spectral frequency components, is given in Fig. 11 for two representative line-averaged densities, $\bar{n}_e = 3.5 \times 10^{12}$ cm^{-3} and 5.5×10^{12} cm^{-3}. This radial flux is always outward and around the LCFS has a value $\Gamma_{\tilde{n}\tilde{\phi}} \approx (3\text{–}4) \times 10^{15}$ cm^{-2}•s^{-1} for $\bar{n}_e = 3.5 \times 10^{12}$ cm^{-3} and $(1\text{–}2) \times 10^{15}$ cm^{-2}•s^{-1} for $\bar{n}_e = 5.5 \times 10^{12}$ cm^{-3}. The corresponding fluctuation-induced particle confinement times, assuming that $\Gamma_{\tilde{n}\tilde{\phi}}$ is toroidally and poloidally uniform on the LCFS, can be estimated from

$$\tau_{\tilde{n}\tilde{\phi}} = (V_p/S_{LCFS}) \langle n_e \rangle_V / \Gamma_{\tilde{n}\tilde{\phi}} = (a/2) \langle n_e \rangle_V / \Gamma_{\tilde{n}\tilde{\phi}}, \tag{4}$$

where (V_p/S_{LCFS}) is the ratio of the core plasma volume to the area of the LCFS, and $\langle n_e \rangle_V$ is the volume-averaged core plasma density. The core density profiles observed in ATF are nearly flat with $\langle n_e \rangle_V \approx \bar{n}_e$. Thus, Eq. (4) yields $\tau_{\tilde{n}\tilde{\phi}} \approx 10\text{–}50$ ms for these line-averaged densities. Although detailed scans of $\bar{n}_e$ have not yet been carried out, results from the present limited scans indicate that $\tau_{\tilde{n}\tilde{\phi}}$ increases with $\bar{n}_e$ in these low-density plasmas. This observation is consistent with the TEXT results.[16]

The associated fluctuation-induced local density diffusion coefficient is $D_n =$

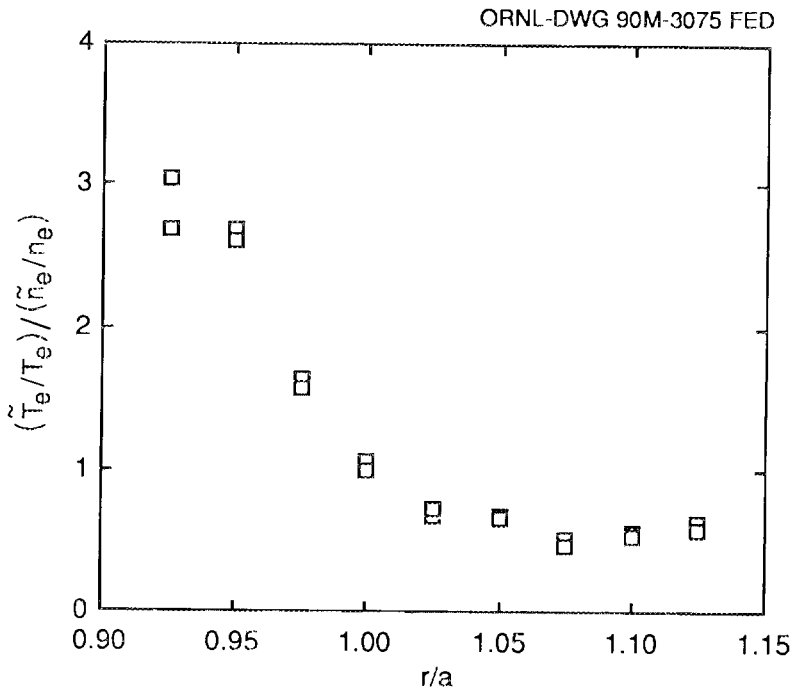

Fig. 8. Estimated edge plasma electron temperature fluctuations $\tilde{T}_e/T_e$ from the triple Langmuir probe measurements, normalized to $\tilde{n}_e/n_e$.

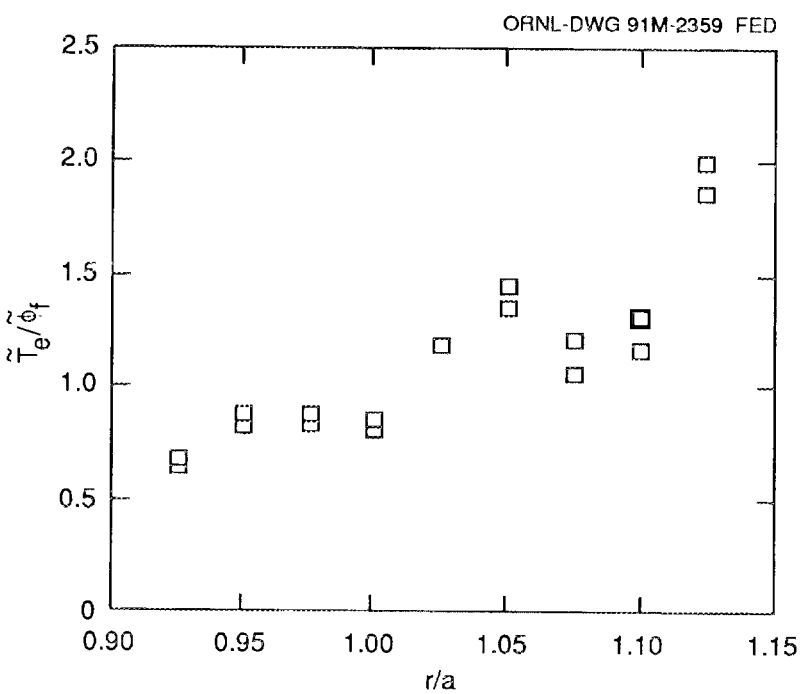

Fig. 9. Edge plasma electron temperature fluctuations, normalized to the floating potential fluctuations $\tilde{T}_e/\tilde{\phi}_f$.

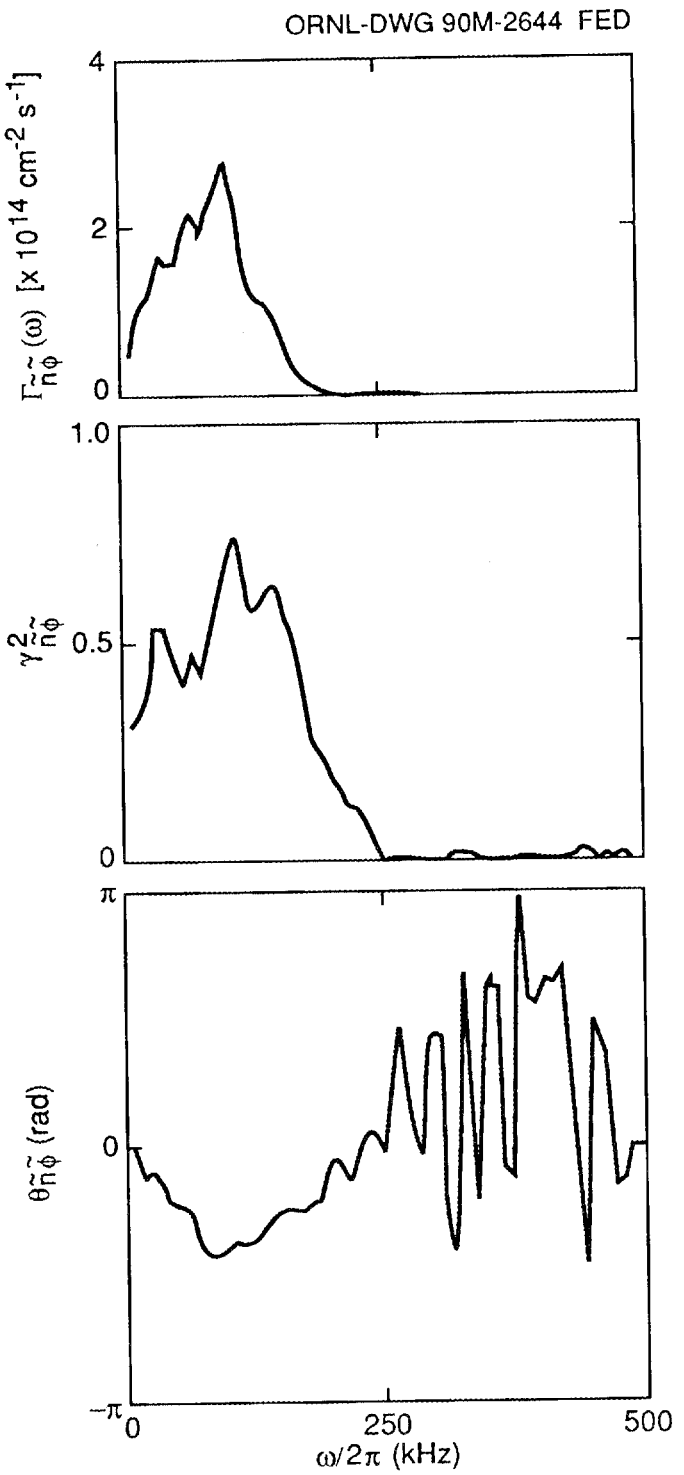

Fig. 10. Typical spectrum of the frequency-resolved particle flux $\Gamma_{\tilde{n}\tilde{\phi}}(\omega)$, the coherence between the density and the floating potential fluctuations $\gamma_{\tilde{n}\tilde{\phi}}$, and the corresponding phase angle $\theta_{\tilde{n}\tilde{\phi}}$.

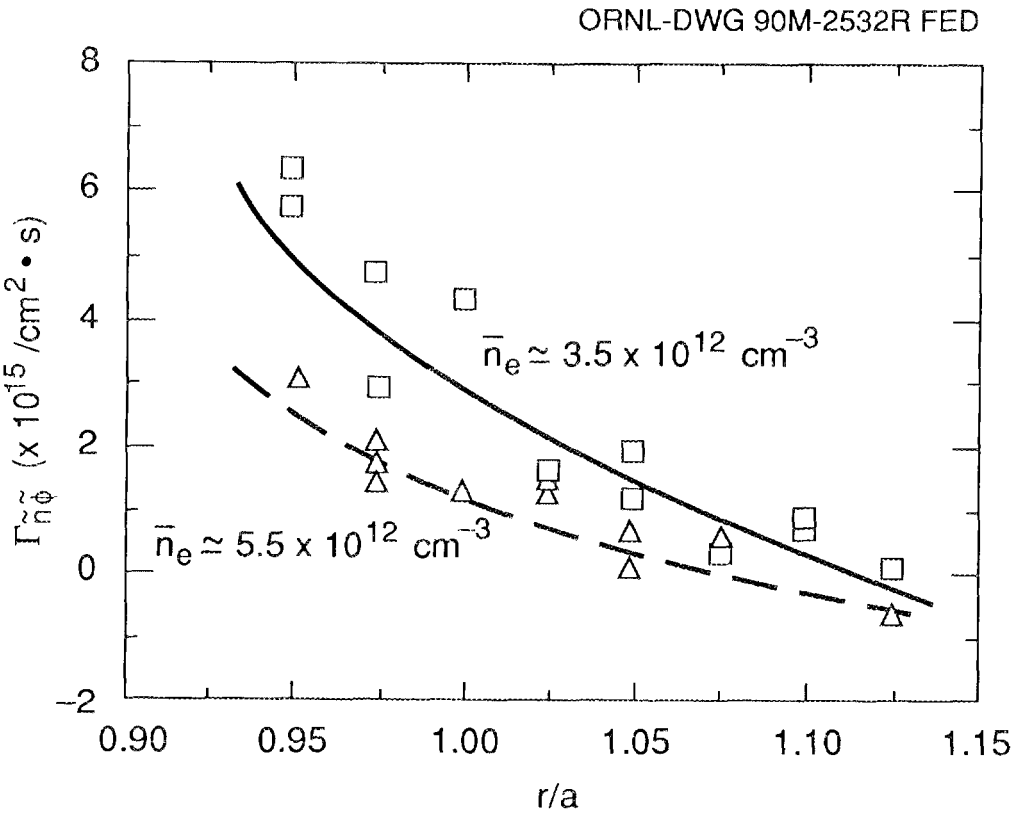

Fig. 11. Spatial profile of the fluctuation-induced particle flux $\Gamma_{\tilde{n}\tilde{\phi}}(\omega)$ at the edge.

$\Gamma_{\tilde{n}\tilde{\phi}} L_n/n_e \approx 1 \times 10^4$ cm^2•s^{-1}, where n_e(edge) $\approx 10^{12}$ cm^{-3} and $L_n \approx 4$ cm for both $\bar{n}_e$ cases. For these discharges, $D_n \leq D_B$ at the LCFS, where D_B (in cm^2•s^{-1}) is the Bohm diffusion coefficient, $D_B = 625 \times T_e/B$ (with T_e in eV and B in T). Estimates of edge particle fluxes from the H_α spectroscopic measurements are rather difficult in ATF because of the lack of a full set of spectroscopic monitors to cover the complicated edge geometry and the existence of particle sources from the divertor stripes[17] around the LCFS. However, some comparisons can be made using the available data.

In steady state, from the particle balance, the edge radial particle flux leaving the core plasma, $r/a \approx 1$, is $\Gamma = \Sigma_j \Phi_j / S_{LCFS}$, where $\Sigma_j \Phi_j$ is the total rate of electron production from ionization of the recycled flux from the walls Φ_W, the limiters Φ_L, and the flux of particles introduced by the gas valve Φ_G. Here again Γ is assumed to be constant on the LCFS. The contributions of the impurities are ignored because of the low Z_{eff} (≈ 1.8). From absolute measurements of H_α radiance in the vicinity of walls (observed vertically and horizontally) and also at the limiter, these fluxes are estimated using a collisional-radiative model[18] to be $\Phi_W = S_W C_{ie} I_\alpha(W)$ and $\Phi_L = S_L C_{ie} I_\alpha(L)$. Here $S_W = 25$ m^2 is the

estimated area of the emitting H_α shell in the vicinity of the walls, S_L is the total area of the top and bottom limiters, which cover about 0.45% of the LCFS area, and C_{ie} ($\approx$ 12 for edge plasmas with $T_e \approx$ 20–30 eV) is the ratio of ionization to excitation events.[18] $I_\alpha(W)$ is the average H_α radiance obtained from the measurements of the vertical and horizontal H_α wall monitors, and $I_\alpha(L)$ is the limiter H_α radiance when the limiter is located at the LCFS. Thus, the estimated radial flux is $\Gamma \approx (1\text{–}1.5) \times 10^{15}$ cm^{-2}•s^{-1} for $\bar{n}_e = 5.5 \times 10^{12}$ cm^{-3}, which is comparable to $\Gamma_{\tilde{n}\tilde{\phi}}$ at the LCFS. This suggests that the electrostatic edge turbulence may play an important role in determining the global particle confinement characteristics in ATF.

A velocity shear layer is observed in the ATF edge; this is also the case in TEXT.[2] Figure 12(a) shows the spatial profile of the mean phase velocity of the fluctuations, $v_{ph} = 2\Sigma_{\omega>0} v_{ph}(\omega)$ with $v_{ph}(\omega) = \Sigma_k(\omega/k)S(k,\omega)/\Sigma_k S(k,\omega)$. The location of the shear layer approximately coincides with the peak of the plasma potential [Fig. 12(b)]. There the radial electric field $E_r = -d\phi_p/dr$ changes its sign and the density and electron temperature gradients are nearly zero, as shown in Fig. 3. Thus $v_{ph} \approx v_{de} \approx 0$, where $v_{de} = (T_e/eB) \times (1/L_n + 1/L_T) - E_r/B$ is the electron drift velocity. Just inside the shear layer a steep density gradient is observed. At $r/a \approx 1.025$, where v_{ph} has its maximum at the electron drift direction, the estimated electric field is $E_r \approx -12$ V/cm, the electron temperature profile is flat with $T_e \approx 30$ eV, and $L_n \approx 4$ cm. The electron drift velocity is then $v_{de} \approx 2.1 \times 10^5$ cm/s, which is comparable to the phase velocity of the fluctuations. Well inside the LCFS, where $E_r \approx 0$, it is estimated that $v_{de} \approx v_{ph} \approx 10^5$ cm/s.

Future experiments will include measurements of the electron temperature fluctuations as described in Refs. 15 and 19 to determine the relationship between $\tilde{\phi}_p/T_e$ and $\tilde{n}_e/n_e$, scaling studies of the edge fluctuation parameters with $\bar{n}_e$, and extension of the ECH experiments to B = 2 T and neutral-beam-heated plasmas. The recently installed heavy ion beam probe diagnostic[20] is expected to provide additional information on the plasma potential and its fluctuations.

IV. CONCLUSION

The initial results indicate substantial similarities in the characteristics of electrostatic edge turbulence in the current-free ATF torsatron and the ohmically heated TEXT tokamak. The fluctuation-induced particle flux is consistent with the total particle flux estimated from the global particle balance (if the fluxes are assumed to be toroidally and poloidally uniform). Thus, electrostatic turbulence may be responsible for the edge particle transport. Detailed comparisons of the ATF and TEXT experimental results are under way.[21] These can serve as a basis for a coherent physics understanding of the effect of edge turbulence on plasma transport in toroidal devices.

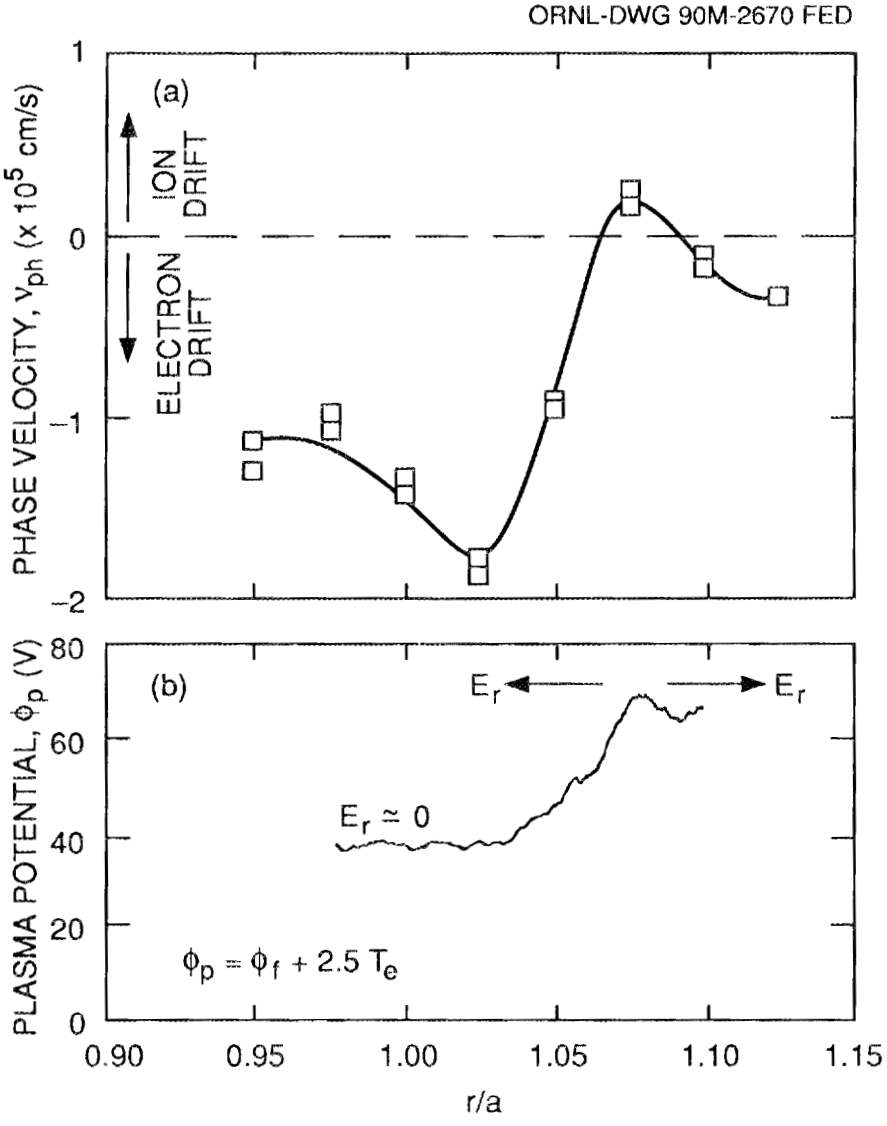

Fig. 12. (a) Spatial profile of the mean phase velocity v_{ph} of the fluctuations. Beyond the shear layer, the wave propagation is in the ion diamagnetic direction. (b) Spatial profile of the estimated edge plasma potential ϕ_p. The shear layer location nearly coincides with the peak of the plasma potential where the radial electric field $E_r = -d\phi_p/dr$ changes its sign.

ACKNOWLEDGMENTS

The authors thank B. A. Carreras, J. N. Leboeuf, P. H. Diamond, and D. R. Thayer for valuable discussions, M. Murakami and the other members of the ATF group and operating staff for help in carrying out the experiments, and J. Sheffield for continual support and encouragement. The authors extend special thanks to K. R. Carter for putting together the FRLP and to G. R. Dyer for the electronics of the probe system.

REFERENCES

1. S. Sudo, Y. Takeiri, H. Zushi, F. Sano, K. Itoh, K. Kondo, and A. Iiyoshi, Nucl. Fusion **30**, 11 (1990).

2. P. Liewer, Nucl. Fusion **15**, 487 (1975).

3. Ch. P. Ritz, R. D. Bengtson, S. J. Levinson, and E. J. Powers, Phys. Fluids **27**, 2956 (1984); Ch. P. Ritz, D. L. Brower, T. L. Rhodes, R. D. Bengtson, S. J. Levinson, N. C. Luhmann, Jr., W. A. Peebles, and E. J. Powers, Nucl. Fusion **27**, 1125 (1987).

4. J. F. Lyon, B. A. Carreras, K. K. Chipley, M. J. Cole, J. H. Harris, T. C. Jernigan, R. L. Johnson, V. E. Lynch, B. E. Nelson, J. A. Rome, J. Sheffield, and P. B. Thompson, Fusion Technol. **10**, 179 (1986).

5. Ch. P. Ritz, R. V. Bravenec, P. M. Schoch, R. D. Bengtson, J. A. Boedo, J. C. Forster, K. W. Gentle, Y. He, R. L. Hickok, Y. J. Kim, H. Lin, P. E. Phillips, T. L. Rhodes, W. L. Rowan, P. M. Valanju, and A. J. Wootton, Phys. Rev. Lett. **62**, 1844 (1989).

6. R. D. Bengtson, K. R. Carter, H. Lin, T. L. Rhodes, Ch. P Ritz, and A. J. Wootton, Bull. Am. Phys. Soc. **32**, 1843 (1987).

7. T. Uckan, P. K. Mioduszewski, D. L. Hillis, C. L. Hahs, W.R. DeVan, J. W. Halliwell, and D. L. Million, Bull. Am. Phys. Soc. **33**, 2069 (1988).

8. E. J. Powers, Nucl. Fusion **14**, 749 (1974).

9. J. M. Beall, Y. C. Kim, and E. J. Powers, J. Appl. Phys. **43**, 3993 (1982).

10. Ch. P. Ritz, E. J. Powers, T. L. Rhodes, R. D. Bengtson, K. W. Gentle, Hong Lin, P. E. Phillips, A. J. Wootton, D. L. Brower, N. C. Luhmann, Jr., W. A. Peebles, P. M. Schoch, and R. L. Hickok, Rev. Sci. Instrum. **59**, 1739 (1988).

11. P.C. Stangeby, Plasma sheath, in Physics of Plasma-Wall Interactions in Controlled Fusion, edited by D. E. Post and R. Behrisch (Plenum, New York, 1986), p. 41.

12. M. Wakatani and A. Hasegawa, Phys. Fluids 27, 611 (1984).

13. A. Carlson, A. Rudyj, and H. Niedermeyer, in Proceedings of the Cadarache Workshop on Electrostatic Turbulence, EUR-CEA-FC-1381 (1989), p. 225.

14. C. Hidalgo, T. Uckan, J. D. Bell, J. H. Harris, B. A. Carreras, J. L. Dunlap, G. R. Dyer, Ch. P. Ritz, A. J. Wootton, T. L. Rhodes, and K. Carter, in Proceedings of the 17th European Conference on Controlled Fusion and Plasma Physics, Amsterdam, 1990 (European Physical Society, 1990), Vol. 14B, Part III, p. 1353.

15. H. Lin, R. D. Bengtson, and Ch. P. Ritz, Phys. Fluids B **1**, 2027 (1989).

16. W. L. Rowan, C. C. Klepper, C. P. Ritz, R. D. Bengtson, K. W. Gentle, P. E. Phillips, T. L. Rhodes, B. Richards, and A. J. Wootton, Nucl. Fusion **27**, 1105 (1987).

17. P. K. Mioduszewski, T. Uckan, D. L. Hillis, J. A. Rome, R. H. Fowler, J. C. Glowienka, M. Murakami, and G. H. Neilson, in Proceedings of the 16th European Conference on Controlled Fusion and Plasma Physics, Venice, 1989 (European Physical Society, 1989), Vol. 13B, Part I, p. 623.

18. L. C. Johnson and E. Hinnov, J. Quant. Spectrosc. Radiat. Transfer **13**, 333 (1973).

19. D. C. Robinson and M. G. Rusbridge, Plasma Phys. **11**, 73 (1969).

20. A. Carnevali, K. A. Connor, S. C. Aceto, J. F. Lewis, J. C. Glowienka, D. Shipley, and C. Eberle, Rev. Sci. Instrum. **59**, 1670 (1988).

21. Ch. P. Ritz, C. Hidalgo, H. Lin, M. Meier, T. L. Rhodes, A. J. Wootton, T. Uckan, J. D. Bell, J. L. Dunlap, J. H. Harris, and G. H. Neilson, Bull. Am. Phys. Soc. **34**, 2153 (1989).

ORNL/TM-11623
Dist. Category UC-426

INTERNAL DISTRIBUTION

1. Director, Fusion Energy Division
2. C. C. Baker
3. M. J. Saltmarsh
4. L. A. Berry
5. B. A. Carreras
6. R. A. Dory
7. J. L. Dunlap
8. H. H. Haselton
9. M. S. Lubell
10. T. E. Shannon

11–12. Laboratory Records Department
13. Laboratory Records, ORNL-RC

14–15. Central Research Library
16. Document Reference Section
17. Fusion Energy Division Library

18–19. Engineering Technology/Fusion Energy Division Publications Office
20. ORNL Patent Office

21–30. T. Uckan
31. J. D. Bell
32. L. A. Charlton
33. R. J. Colchin
34. G. R. Dyer
35. G. R. Hanson
36. J. H. Harris
37. D. L. Hillis
38. S. Hiroe
39. L. D. Horton
40. R. C. Isler
41. T. C. Jernigan
42. J. N. Leboeuf
43. J. F. Lyon
44. P. K. Mioduszewski
45. M. Murakami
46. D. A. Rasmussen
47. K. C. Shaing
48. J. B. Wilgen
49. W. R. Wing

EXTERNAL DISTRIBUTION

50. Office of the Assistant Manager for Energy Research and Development, U.S. Department of Energy, Oak Ridge Operations Office, P.O. Box E, Oak Ridge, TN 37831
51. J. D. Callen, Department of Nuclear Engineering, University of Wisconsin, Madison, WI 53706-1687
52. R. W. Conn, Department of Chemical, Nuclear, and Thermal Engineering, University of California, Los Angeles, CA 90024

53. N. A. Davies, Acting Director, Office of Fusion Energy, Office of Energy Research, ER-50 Germantown, U.S. Department of Energy, Washington, DC 20545
54. S. O. Dean, Fusion Power Associates, Inc., 2 Professional Drive, Suite 248, Gaithersburg, MD 20879
55. H. K. Forsen, Bechtel Group, Inc., Research Engineering, P.O. Box 3965, San Francisco, CA 94119
56. R. W. Gould, Department of Applied Physics, California Institute of Technology, Pasadena, CA 91125
57. R. A. Gross, Plasma Research Laboratory, Columbia University, New York, NY 10027
58. D. M. Meade, Princeton Plasma Physics Laboratory, P.O. Box 451, Princeton, NJ 08543
59. M. Roberts, International Programs, Office of Fusion Energy, Office of Energy Research, ER-52 Germantown, U.S. Department of Energy, Washington, DC 20545
60. W. M. Stacey, School of Nuclear Engineering and Health Physics, Georgia Institute of Technology, Atlanta, GA 30332
61. D. Steiner, Nuclear Engineering Department, NES Building, Tibbetts Avenue, Rensselaer Polytechnic Institute, Troy, NY 12181
62. R. Varma, Physical Research Laboratory, Navrangpura, Ahmedabad 380009, India
63. Bibliothek, Max-Planck Institut für Plasmaphysik, Boltzmannstrasse 2, D-8046 Garching, Federal Republic of Germany
64. Bibliothek, Institut für Plasmaphysik, KFA Jülich GmbH, Postfach 1913, D-5170 Jülich, Federal Republic of Germany
65. Bibliothek, KfK Karlsruhe GmbH, Postfach 3640, D-7500 Karlsruhe 1, Federal Republic of Germany
66. Bibliothèque, Centre de Recherches en Physique des Plasmas, Ecole Polytechnique Fédérale de Lausanne, 21 Avenue des Bains, CH-1007 Lausanne, Switzerland
67. J. Tachon, CEN/Cadarache, Departement de Recherches sur la Fusion Contrôlée, F-13108 Saint-Paul-lez-Durance Cedex, France
68. Bibliothèque, CEN/Cadarache, F-13108 Saint-Paul-lez-Durance Cedex, France
69. Library, AEA Fusion, Culham Laboratory, Abingdon, Oxfordshire, OX14 3DB, England
70. Library, JET Joint Undertaking, Abingdon, Oxfordshire OX14 3EA, England
71. Library, FOM-Instituut voor Plasmafysica, Rijnhuizen, Edisonbaan 14, 3439 MN Nieuwegein, The Netherlands
72. Library, National Institute for Fusion Science, Chikusa-ku, Nagoya 464-01, Japan
73. Library, International Centre for Theoretical Physics, P.O. Box 586, I-34100 Trieste, Italy
74. Library, Centro Richerche Energia Frascati, C.P. 65, I-00044 Frascati (Roma), Italy
75. Library, Plasma Physics Laboratory, Kyoto University, Gokasho, Uji, Kyoto 611, Japan
76. Plasma Research Laboratory, Australian National University, P.O. Box 4, Canberra, A.C.T. 2601, Australia
77. Library, Japan Atomic Energy Research Institute, Naka Fusion Research Establishment, 801-1 Mukoyama, Naka-machi, Naka-gun, Ibaraki-ken, Japan
78. G. A. Eliseev, I. V. Kurchatov Institute of Atomic Energy, P.O. Box 3402, 123182 Moscow, U.S.S.R.
79. V. A. Glukhikh, Scientific-Research Institute of Electro-Physical Apparatus, 188631 Leningrad, U.S.S.R.
80. I. Shpigel, Institute of General Physics, U.S.S.R. Academy of Sciences, Ulitsa Vavilova 38, Moscow, U.S.S.R.
81. D. D. Ryutov, Institute of Nuclear Physics, Siberian Branch of the Academy of Sciences of the U.S.S.R., Sovetskaya St. 5, 630090 Novosibirsk, U.S.S.R.
82. O. Pavlichenko, Kharkov Physical-Technical Institute, Academical St. 1, 310108 Kharkov, U.S.S.R.
83. Deputy Director, Southwestern Institute of Physics, P.O. Box 15, Leshan, Sichuan, China (PRC)
84. Director, The Institute of Plasma Physics, P.O. Box 26, Hefei, Anhui, China (PRC)

85. R. A. Blanken, Experimental Plasma Physics Research Branch, Division of Applied Plasma Physics, Office of Energy Research, ER-542, Germantown, U.S. Department of Energy, Washington, DC 20545
86. R. A. E. Bolton, IREQ Hydro-Quebec Research Institute, 1800 Montée-Ste.-Julie, Varennes, P.Q. JOL 2P0, Canada
87. D. H. Crandall, Experimental Plasma Physics Research Branch, Division of Applied Plasma Physics, Office of Energy Research, ER-542, Germantown, U.S. Department of Energy, Washington, DC 20545
88. R. L. Freeman, General Atomics, P.O. Box 85608, San Diego, CA 92138-5608
89. K. W. Gentle, RLM 11.222, Institute for Fusion Studies, University of Texas, Austin, TX 78712
90. R. J. Goldston, Princeton Plasma Physics Laboratory, P.O. Box 451, Princeton, NJ 08543
91. J. C. Hosea, Princeton Plasma Physics Laboratory, P.O. Box 451, Princeton, NJ 08543
92. D. Markevich, Division of Confinement Systems, Office of Energy Research, ER-55, Germantown, U.S. Department of Energy, Washington, DC 20545
93. R. H. McKnight, Experimental Plasma Physics Research Branch, Division of Applied Plasma Physics, Office of Energy Research, ER-542, Germantown, U.S. Department of Energy, Washington, DC 20545
94. E. Oktay, Division of Confinement Systems, Office of Energy Research, ER-55, Germantown, U.S. Department of Energy, Washington, DC 20545
95. R. R. Parker, Plasma Fusion Center, NW 16-288, Massachusetts Institute of Technology, Cambridge, MA 02139
96. W. L. Sadowski, Fusion Theory and Computer Services Branch, Division of Applied Plasma Physics, Office of Energy Research, ER-541, Germantown, U.S. Department of Energy, Washington, DC 20545
97. J. W. Willis, Division of Confinement Systems, Office of Energy Research, ER-55, Germantown, U.S. Department of Energy, Washington, DC 205
98. A. Perez Navarro, Division de Fusion, CIEMAT, Avenida Complutense 22, E-28040 Madrid, Spain
99. Laboratory for Plasma and Fusion Studies, Department of Nuclear Engineering, Seoul National University, Shinrim-dong, Gwanak-ku, Seoul 151, Korea
100. J. L. Johnson, Plasma Physics Laboratory, Princeton University, P.O. Box 451, Princeton, NJ 08543
101. L. M. Kovrizhnykh, Institute of General Physics, U.S.S.R. Academy of Sciences, Ulitsa Vavilova 38, 117924 Moscow, U.S.S.R.
102. O. Motojima, National Institute for Fusion Science, Chikusa-ku, Nagoya 464-01, Japan
103. S. Okamura, Institute of Plasma Physics, Nagoya University, Chikusa-ku, Nagoya 464, Japan
104. V. D. Shafranov, I. V. Kurchatov Institute of Atomic Energy, P.O. Box 3402, 123182 Moscow, U.S.S.R.
105. J. L. Shohet, Torsatron/Stellarator Laboratory, University of Wisconsin, Madison, WI 53706
106. H. Wobig, Max-Planck Institut für Plasmaphysik, D-8046 Garching, Federal Republic of Germany
107. E. Anabitarte, Avenida de los Castros s/n, Dept. de Fisica Applicada, Universidad de Cantabria, 39005 Santander, Spain
108. F. S. B. Anderson, University of Wisconsin, Madison, WI 53706
109. R. F. Gandy, Physics Department, Auburn University, Auburn, AL 36849-3511
110. C. Hidalgo-Vera, Division de Fusion, CIEMAT, Avenida Complutense 22, E-28040 Madrid, Spain
111. H. Kaneko, Plasma Physics Laboratory, Kyoto University, Gokasho, Uji, Japan
112. G. H. Neilson, Princeton Plasma Physics Laboratory, P.O. Box 451, Princeton, NJ 08543
113. Ch. P. Ritz, Fusion Research Center, University of Texas, Austin, TX 78712
114. S. Sudo, Plasma Physics Laboratory, Kyoto University, Gokasho, Uji, Japan
115. C. E. Thomas, Georgia Institute of Technology, Atlanta, GA 30332
116. H. Yamada, National Institute for Fusion Science, Chikusa-ku, Nagoya 464-01, Japan

117. F. W. Perkins, Princeton Plasma Physics Laboratory, P.O. Box 451, Princeton, NJ 08543
118. T. Obiki, Plasma Physics Laboratory, Kyoto University, Gokasho, Uji, Kyoto, Japan
119. A. Iiyoshi, National Institute for Fusion Studies, Chikusa-ku, Nagoya 464-01, Japan
120. T. L. Rhodes, Fusion Research Center, University of Texas, Austin, TX 78712
121. A. J. Wootton, Fusion Research Center, University of Texas, Austin, TX 78712

122–174. Given distribution as shown in OSTI-4500, Magnetic Fusion Energy (Category Distribution UC-426, Experimental Plasma Physics) (53 copies)